lent Reacting Multi-Phase Flows," *4th International Symposium on Transport Phenomena in Heat and Mass Transfer* (Sydney, Australia), Vol. 1, 1991, pp. 391-401.

[13]Chan, S. H., and Tan, C. C., "Complex Equilibrium Calculation by Simplex and Duality Theories with Applications to Liquid Metal Fuel Propulsion Systems," *Combustion and Flame,* Vol. 88, Feb. 1992, pp. 123-136.

[14]Parnell, L. A., Gilchrist, J. T., and Rogerson, D. J., "Flash and Real-Time Radiographic Study of Closed Liquid Metal Combustion," *2nd Office of Naval Research Propulsion Meeting* (Irvine, CA), Oct. 1989, pp. 188-205.

Initial Acceleration Effects on Flow Evolution Around Airfoils Pitching to High Angles of Attack

Manoochehr M. Koochesfahani* and
Vanco Smiljanovski†
Michigan State University,
East Lansing, Michigan 48824

Introduction

AIRFOILS pitching rapidly to high angles of attack, and the accompanying phenomenon of dynamic stall, were first investigated for the case of sinusoidal motions. The progress in this area is reviewed by McCroskey[1] and Carr.[2] More recently, constant pitch rate (i.e., ramp) motions have been receiving a great deal of attention due to their applicability to supermaneuverable aircraft. Some of the earlier measurements of integrated load[3-5] have now been complemented by computational results[6,7] and high-resolution surface pressure measurements[8]; whole-field velocity information is also becoming available.[9]

Investigations into airfoils pitching at constant rate have typically considered airfoils pitching from a zero angle of attack to some large angle α_{max} well beyond the static stall angle. It has been established that a major parameter governing the flow behavior is the nondimensional pitch rate $\Omega^* = \dot{\alpha}C/(2U_\infty)$, where $\dot{\alpha}$ is the constant pitch rate, C the chord, and U_∞ the freestream speed. It is clear that, in reality, the actual motion of the airfoil must deviate from the ideal ramp due to the finite acceleration and deceleration periods imposed by the damping of the drive system and the response characteristics of the airfoil. The computations of "nominally" constant pitch rate motions also include a brief initial acceleration period. To our knowledge, a systematic investigation of the effects of initial acceleration on the flow characteristics of an airfoil pitching to high angles of attack has not been undertaken. We note that studying such effects can provide not only further insight into the processes of vorticity generation and accumulation on unsteady surfaces, but also clues as to how these processes may be modified or controlled by the deliberate shaping of the pitch-motion trajectory.

In the present experiments, flow visualization is used to monitor the onset of leading-edge separation and the subsequent dynamic stall vortex development as the initial acceleration is systematically varied in magnitude and duration through the acceleration phase to constant pitch rate. The work presented here considers the case of incompressible flow at low-chord Reynolds numbers and relatively high pitch rate.

Received Oct. 13, 1992; revision received Feb. 10, 1993; accepted for publication Feb. 10, 1993.

*Associate Professor, Department of Mechanical Engineering. Member AIAA.

†Graduate Assistant, Exchange Student, Rheinisch Westfälische Technische Hochschule, Aachen, Germany.

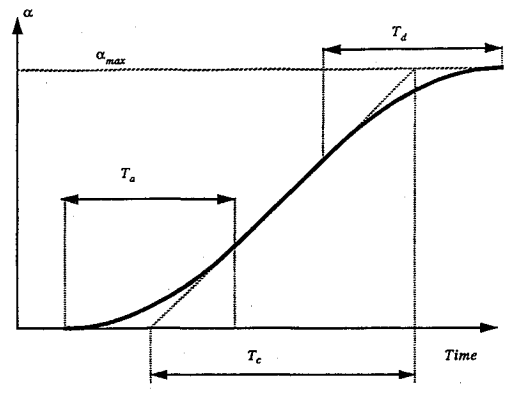

a) Definition sketch; $e \equiv T_a/T_c$

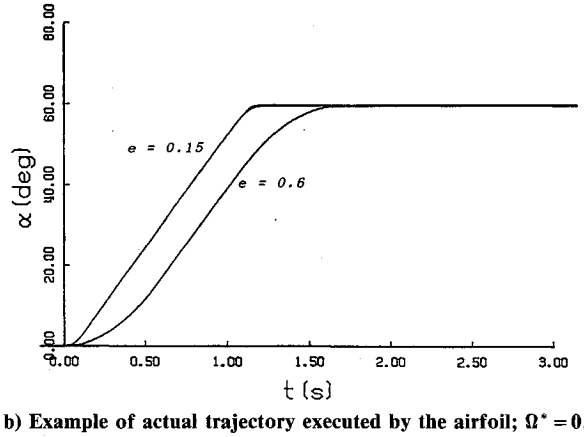

b) Example of actual trajectory executed by the airfoil; $\Omega^* = 0.4$

Fig. 1 Constant pitch rate motion with finite acceleration and deceleration.

Experimental Setup

The experiments were performed in a water channel (Engineering Laboratory Design, Inc.) with a test section 60 × 60 cm in cross section and 240 cm in length. The airfoil was an NACA 0012 with a uniform chord of $C = 8$ cm, a span of $b = 45$ cm, and was fitted on both ends with false walls parallel to the water channel walls. For the results described here, the freestream seed was set to $U_\infty = 10$ cm/s resulting in a chord Reynolds number of 8×10^3. A dc servo motor and a digitial servo controller (Galil, DMC-610) were used to pitch the airfoil about the quarter chord. The pitch-motion trajectory started at zero angle of attack, reached the desired constant pitch rate of $\dot{\alpha}$ after a period T_a of constant acceleration, and stopped at the final angle of attack of 60 deg after a period T_d of constant deceleration (see Fig. 1a). The acceleration and deceleration periods were kept equal in this work. We characterize the pitch trajectory by the nondimensional pitch rate Ω^* and an acceleration parameter $e = T_a/T_c$, where T_c is the "ideal" constant pitch rate time scale needed for the motion. Note that the parameter e gives an indication of the fraction of the motion time used for acceleration/deceleration. The particular cases considered in this study correspond to ($\Omega^* = 0.4$; $e = 0.6$, 0.15, 0.037) and ($\Omega^* = 0.2$; $e = 0.15$, 0.037). Typical examples of the actual pitch trajectory executed by the airfoil are shown in Fig. 1b.

The evolution of the flow was monitored using the hydrogen-bubble technique and laser sheet illumination at the airfoil midspan location. The hydrogen-bubble wire was placed approximately 1 mm upstream of the airfoil leading edge and was pulsed at 20 Hz. Flow images were sensed by a charge coupled device camera at a rate of 60 fields/s with an exposure time of 2 ms/field and acquired by a digital image acquisition system (Recognition Concepts, Inc., TRAPIX-5500) onto a hard disk in real time.

Results and Discussion

The evolution of the flowfield for the case ($\Omega^* = 0.4$; $e = 0.15$) is illustrated in Fig. 2. For each picture, the instantaneous angle of attack and the elapsed time from the start of the motion are indicated. The flow follows the contour of the airfoil, and in that sense appears fully attached, up to an angle of attack $\alpha = 27$ deg. By the time the airfoil has reached $\alpha = 34$ deg, leading-edge separation and vortex formation have already begun with a visual signature of a perturbation near the leading edge. The first visual indication of onset of leading-edge separation and vortex formation was found to occur at ($T_s = 0.64$ s; $\alpha_s = 32$ deg) after close inspection of the image time sequence; T_s and α_s refer to the elapsed time and angle of attack at the onset of leading-edge separation. It should be noted that, based on the image acquisition rate, we estimate the value of α_s to ± 1 deg accuracy. The sequence of pictures in Fig. 2 also shows how the leading-edge vortex grows in time and evolves into the dynamic stall vortex. The flow evolution shown in this figure, including the formation of multiple large-scale vortices above the suction surface, is similar to the known computational and experimental results.

The effect of initial acceleration period on the onset of leading-edge separation for the cases considered here were determined from data similar to Fig. 2. The results are summarized in Table 1.

The results show that the onset of leading-edge separation is delayed to a larger angle of attack as the pitch rate increases. This is consistent with the well-established dynamic stall delay for increasing pitch rate.[1-9] The most important observation, however, is that while the elasped time for leading-edge separation and vortex formation is affected by initial acceleration, the angle of attack where this occurs remains virtually unchanged. In fact, many of the details of subsequent flow development are also nearly the same. Figure 3 shows a comparison at selected angles of attack for two cases with $\Omega^* = 0.4$ and initial accelerations which are different by a factor of 4. Note the similarity of the various events at similar angles of attack; there is, of course, a time shift between the occurrence of similar events in the two cases, as indicated earlier.

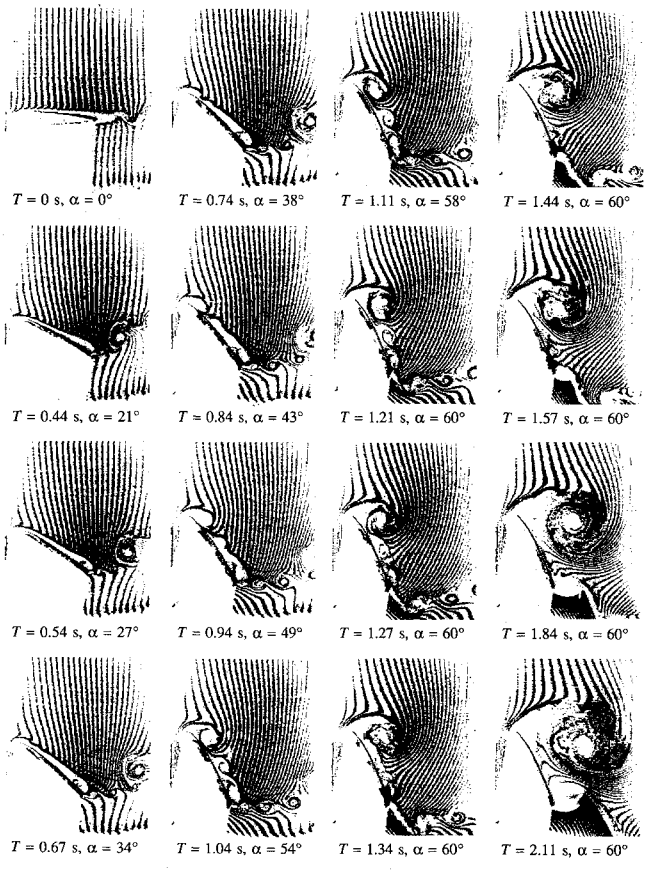

Fig. 2 Evolution of the flowfield on the airfoil suction surface ($\Omega^* = 0.4$, $e = 0.15$).

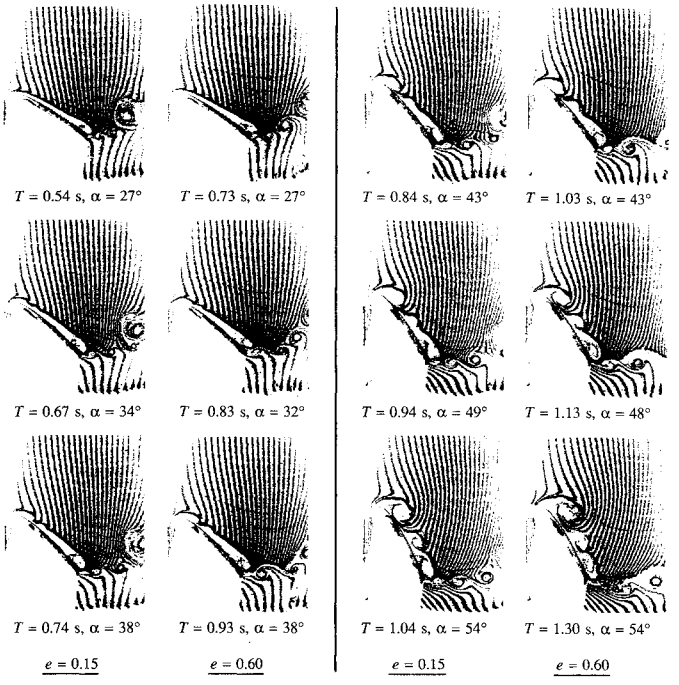

Fig. 3 Comparison of flow evolution for two different initial acceleration periods ($\Omega^* = 0.4$).

Table 1 Time and angle of attack at the onset of leading-edge separation

	T_s, s	α_s, deg
$\Omega^* = 0.4$; $e = 0.6$	0.80	31
$\Omega^* = 0.4$; $e = 0.15$	0.64	32
$\Omega^* = 0.4$; $e = 0.037$	0.57	31
$\Omega^* = 0.2$; $e = 0.15$	0.97	24
$\Omega^* = 0.2$; $e = 0.037$	0.90	25

The downstream convection of the dynamic stall vortex was determined for all of the cases from image sequences similar to Fig. 2. The vortex downstream position X (along freestream direction) was estimated using the center of the nearly circular region interpreted to be the signature of the dynamic stall vortex (e.g., see Fig. 2). The results are referenced to the fixed pitch axis location X_p and are plotted in Fig. 4. Note that the differences in the times for the onset of leading-edge separation among the various cases have been taken into account by using the relative time ($T - T_s$). The main result from Fig. 4 is that the initial acceleration period also has little influence on the downstream convection of the dynamic stall vortex for the cases studied. Note that the vortex convection speed U_c/U_∞ (determined from a least-squares straight line fit to data) is 0.44 and 0.40 for $\Omega^* = 0.4$ and 0.20, respectively.

To summarize, the results presented indicate that the elapsed time for the occurrence of various events is affected by the initial acceleration; the angle of attack where these events occur is practically unchanged, however. This includes the onset of leading-edge separation and many of the details of the dynamic stall vortex formation, downstream convection, and its interactions. These results imply that a convenient acceleration profile can be selected for experimental and computational studies without seriously impacting the dynamics of the unsteady stall process.

A scaling argument based on unsteady inviscid flow results had earlier suggested[10] that if the initial acceleration time scale is sufficiently short compared to the flow time scale, the onset

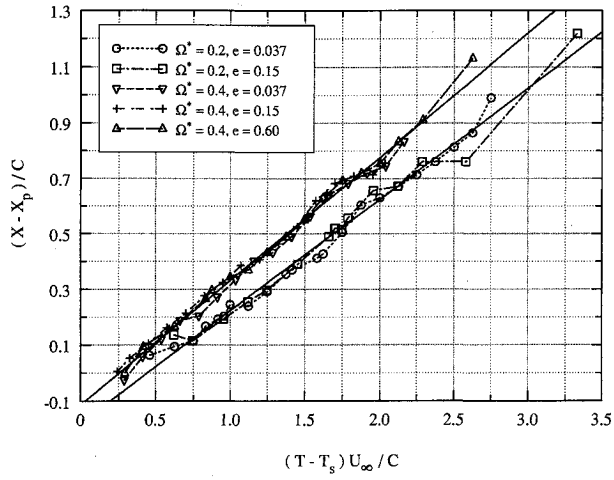

Fig. 4 Downstream convection of the dynamic stall vortex. Solid lines represent the least-squares line fit to data.

of leading-edge separation might be expected to be insensitive to the motion history, as is resported here. This is consistent with the constant pitch rate, inviscid flow, lift-curve slope results in Ref. 4 which indicate that at high enough pitch rates motion history effects will saturate. We should mention that in all of the cases studied here, the acceleration period was short enough that it ended before the onset of leading-edge separation. Reference 10 further suggests that initial acceleration effects may become important for a combination of low pitch rate Ω^* and long acceleration period e.

We note that the results presented here only address the timing of the various events in the flowfield development. We do not know at this time how other important quantities such as the surface pressure gradient, surface vorticity flux, and the integrated load on the airfoil are affected as we change the acceleration period. These questions are currently being addressed by computing the flows discussed here using a two-dimensional Navier-Stokes solver. Preliminary computational results[11] corroborate the present findings.

Acknowledgments

This work was supported by the Air Force Office of Scientific Research Grants AFOSR-89-0417 and AFOSR-89-0130. Charles Gendrich is gratefully acknowledged for his help with the preparation of the manuscript.

References

[1]McCroskey, W. J., "Unsteady Airfoils," *Annual Review of Fluid Mechanics,* Vol. 14, 1982, pp. 285–311.

[2]Carr, L. W., "Progress in Analysis and Prediction of Dynamic Stall," *Journal of Aircraft,* Vol. 25, No. 1, 1988, pp. 6–17.

[3]Francis, M. S., and Keesee, J. E., "Airfoil Dynamic Stall Performance with Large-Amplitude Motions," *AIAA Journal,* Vol. 23, No. 11, 1985, pp. 1653–1659.

[4]Jumper, E. J., Shreck, S. J., and Dimmick, R. L., "Lift-Curve Characteristics for an Airfoil Pitching at Constant Rate," *Journal of Aircraft,* Vol. 24, No. 10, 1987, pp. 680–687.

[5]Lorber, P. F., and Carta, F. O., "Airfoil Dynamic Stall at Constant Pitch Rate and High Reynolds Number," *Journal of Aircraft,* Vol. 25, No. 6, 1988, pp. 548–556.

[6]Visbal, M. R., "On the Formation and Control of the Dynamic Stall Vortex on a Pitching Airfoil," AIAA Paper 91-0006, Jan. 1991.

[7]Ghia, K. N., Yang, J., Osswald, G. A., and Ghia, U., "Study of the Dynamic Stall Mechanism Using Simulation of Two-Dimensional Navier-Stokes Equations," AIAA Paper 91-0546, Jan. 1991.

[8]Acharya, M., and Metwally, M. H., "Unsteady Pressure Field and Vorticity Production over a Pitching Airfoil," *AIAA Journal,* Vol. 30, No. 2, 1992, pp. 403–411.

[9]Shih, C., Lourenco, L., Van Dommelen, L., and Krothapalli, A., "Unsteady Flow Past an Airfoil Pitching at Constant Rate," *AIAA Journal,* Vol. 30, No. 5, 1992, pp. 1153–1161.

[10]Koochesfahani, M. M., Smiljanovski, V., and Brown, T. A., "Effect of Initial Acceleration on the Flow Development of the Flow Field of an Airfoil Pitching at Constant Rate," *Proceedings of NASA/AFOSR/ARO Workshop on Physics of Forced Unsteady Separation,* NASA Ames Research Center, April 17–19, 1990, NASA CP 3144, 1992, pp. 317–332.

[11]Gendrich, C. P., Koochesfahani, M. M., and Visbal, M. R., "Initial Acceleration Effects on the Flow Field Development around Rapidly Pitching Airfoils," AIAA Paper 93-0438, Jan. 1993.

Decay of Aircraft Vortices near the Ground

Milton E. Teske* and Alan J. Bilanin†
Continuum Dynamics, Inc., Princeton, New Jersey 08543
and
John W. Barry‡
U.S. Department of Agriculture Forest Service, Davis, California 95616

Introduction

In a review of the state of knowledge of aircraft vortices, Donaldson and Bilanin[1] include a discussion on the effects of atmospheric turbulence on the aging of vortex pairs. One of the models suggested may be written

$$\Gamma(t) = \Gamma_o \exp\left(-\frac{bqt}{s}\right) \tag{1}$$

where Γ is the vortex circulation strength as a function of time t, Γ_o the initial vortex circulation strength at $t = 0$, b the decay coefficient, q the ambient turbulence level, and s the aircraft semispan.

Donaldson and Bilanin[1] invoke simple arguments to suggest that the decay coefficient—out of ground effect—may take a value of 0.41. When details about the wakes of large aircraft were first investigated (in the early 1970s), more sophisticated models, using various techniques such as second-order closure of the Reynolds stress equations,[2] were developed with an eye toward examining this decay behavior. Recently, for a completely different reason, the problem of quantifying the decay coefficient has produced a sizable field study and data examination.

Discussion

Between 1985 and 1991, a series of aircraft flybys above tower grids instrumented with propeller anemometers produced a large data base on vortex motion near the ground.[3] These tests were performed jointly by the United States Department of Agriculture Forest Service and the United States Army at several sites in northern California (through Project WIND), and at Dugway Proving Ground, Utah. Anemometer tower grids recorded the ambient vertical velocity time histories as various aircraft repeatedly traversed normal to the grid. These digitized velocity traces produced an aircraft wake signature that could be used to infer the strength and lateral and vertical motion of the aircraft vortex pairs generating the traces. Table 1 summarizes the complete data set.

The location and strength of the vortices traversing the anemometer tower grid may be inferred by a least-squares analysis defining an error E as

$$E = \sum_{n=1}^{N} (w_n - \bar{w}_n)^2 \tag{2}$$

Received Nov. 12, 1992; revision received Jan. 15, 1993; accepted for publication Feb. 5, 1993.

*Senior Associate, P.O. Box 3073.
†President and Senior Associate, P.O. Box 3073.
‡Pesticide Specialist, Forest Pest Management, 2121C Second Street, Suite 102.